

Beacons into the Cosmic Dark Ages: Boosted transmission of Ly α from UV bright galaxies at $z \gtrsim 7$

CHARLOTTE A. MASON¹, TOMMASO TREU¹, STEPHANE DE BARROS^{2,3}, MARK DIJKSTRA⁴, ADRIANO FONTANA⁵,
ANDREI MESINGER⁶, LAURA PENTERICCI⁵, MICHELE TRENTI^{7,8}, AND EROS VANZELLA³,

¹ Department of Physics and Astronomy, UCLA, Los Angeles, CA, 90095-1547, USA

² Observatoire de Genève, Université de Genève, 51 Ch. des Maillettes, 1290 Versoix, Switzerland

³ INAF Osservatorio Astronomico di Bologna, via Gobetti 93/3, 40129 Bologna, Italy

⁴ Institute of Theoretical Astrophysics, University of Oslo, P.O. Box 1029, N-0315 Oslo, Norway

⁵ INAF Osservatorio Astronomico di Roma, Via Frascati 33, I-00040 Monteporzio (RM), Italy

⁶ Scuola Normale Superiore, Piazza dei Cavalieri 7, I-56126 Pisa, Italy

⁷ School of Physics, University of Melbourne, Parkville, Victoria, Australia and

⁸ ARC Centre of Excellence for All Sky Astrophysics in 3 Dimensions (ASTRO 3D)

Draft version November 4, 2021

Abstract

Recent detections of Lyman alpha (Ly α) emission from $z > 7.5$ galaxies were somewhat unexpected given a dearth of previous non-detections in this era when the intergalactic medium (IGM) is still highly neutral. But these detections were from UV bright galaxies, which preferentially live in overdensities which reionize early, and have significantly Doppler-shifted Ly α line profiles emerging from their interstellar media (ISM), making them less affected by the global IGM state. Using a combination of reionization simulations and empirical ISM models we show, as a result of these two effects, UV bright galaxies in overdensities have $> 2\times$ higher transmission through the $z \sim 7$ IGM than typical field galaxies, and this boosted transmission is enhanced as the neutral fraction increases. The boosted transmission is not sufficient to explain the observed high Ly α fraction of $M_{UV} \lesssim -22$ galaxies (Stark et al. 2017), suggesting Ly α emitted by these galaxies must be stronger than expected due to enhanced production and/or selection effects. Despite the bias of UV bright galaxies to reside in overdensities we show Ly α observations of such galaxies can accurately measure the global neutral hydrogen fraction, particularly when Ly α from UV faint galaxies is extinguished, making them ideal candidates for spectroscopic follow-up into the cosmic Dark Ages.

Subject headings: dark ages, reionization, first stars — galaxies: high-redshift — galaxies: evolution — intergalactic medium

1. Introduction

Reionization of hydrogen in the universe’s first billion years was driven by the first sources of light. Accurately measuring the timeline of reionization, i.e. average neutral hydrogen fraction (\bar{x}_{HI}) as a function of redshift, enables us to infer properties of these sources. Ly α emission from galaxies has long been touted as a tracer of \bar{x}_{HI} during reionization: Ly α photons are absorbed by neutral hydrogen (e.g., Dijkstra 2014).

The rapidly declining fraction of Lyman-break galaxies (LBGs) emitting Ly α at $z > 6$ (e.g., Fontana et al. 2010; Stark et al. 2010; Treu et al. 2013; Schenker et al. 2014; Pentericci et al. 2014; Mason et al. 2018) and strong damping wing absorption of $z \sim 7$ quasar spectra (Greig et al. 2016; Bañados et al. 2017) suggest the universe is significantly neutral at $z \gtrsim 7$. Recent detections of Ly α from galaxies at $z > 7.5$ (Roberts-Borsani et al. 2016; Zitrin et al. 2015; Oesch et al. 2015; Stark et al. 2017) are therefore surprising. Furthermore, these detections come from $M_{UV} \lesssim -22$ galaxies ($\gtrsim 2.5L^*$). At lower redshifts UV bright galaxies are least likely to have strong Ly α (e.g. Stark et al. 2010). Why can we see Ly α from these galaxies?

Reionization is likely highly inhomogeneous – over-

dense regions reionize more rapidly as they are filled with many ionizing sources (e.g., McQuinn et al. 2007). The brightest galaxies likely reside in overdensities (e.g., Trenti et al. 2012; Barone-Nugent et al. 2014; Castellano et al. 2016). How easily are Ly α photons from such galaxies in overdensities transmitted through the IGM, compared to field galaxies? How does the ISM radiative transfer of Ly α affect its IGM transmission? (Figure 1) Can these biased galaxies still measure \bar{x}_{HI} ?

Here we combine cosmological reionization simulations with empirical models of galaxy properties to understand the transmission of Ly α from UV bright galaxies. We describe our combination of simulations and empirical models in Section 2. In Section 3 we present our results on the evolving transmission of Ly α emission from galaxies in massive halos, the interpretation of the observed ‘Ly α fraction’, and the efficacy of UV bright galaxies as probes of \bar{x}_{HI} . We discuss our results in Section 4 and summarize in Section 5.

We use the Planck Collaboration et al. (2015) cosmology. All magnitudes are in the AB system.

2. Method

To model the transmission of Ly α photons from galaxies through the reionizing IGM we combine the public

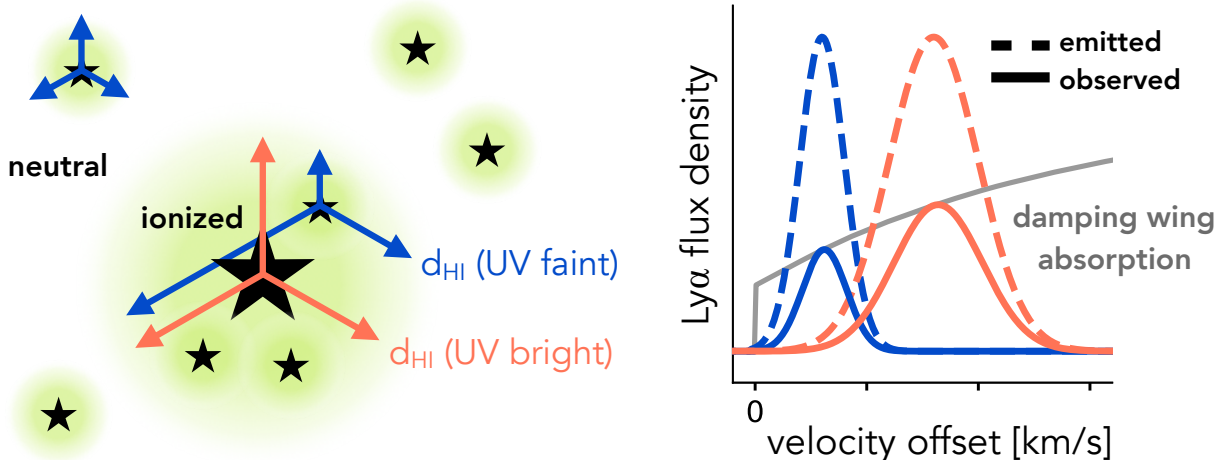


FIG. 1.— **Left:** UV bright galaxies (large stars) preferentially live in overdensities, which reionize early (green regions). Ly α damping wing optical depths are dominated by the distance to the first neutral patch (white regions) photons encounter, d_{HI} , thus UV bright galaxies have higher average Ly α transmission than UV faint galaxies (small stars) as they live further from neutral patches. The sightline-to-sightline scatter of Ly α transmissions for UV bright galaxies is lower due to lower scatter in d_{HI} (orange arrows for UV bright galaxies, blue arrows for UV faint galaxies). **Right:** Gas and dust resonantly scatter and absorb Ly α photons inside galaxies. Ly α emitted (dashed lines) by UV bright galaxies (orange) is usually more Doppler-shifted than Ly α from UV faint galaxies (blue), as they contain more gas and dust. Damping wing absorption during reionization attenuates Ly α smoothly with wavelength/velocity offset (gray line – example shown is $\bar{x}_{\text{HI}} = 0.66$), so Ly α transmitted (solid lines) through the IGM depends on galaxy properties.

Evolution of Structure simulations (EoS¹, Mesinger et al. 2016) with empirical models of galaxy properties. We follow the method of Mason et al. (2018) (hereafter M18) and refer the reader there for more details. We describe our methods briefly below.

The EoS simulations treat inhomogeneous recombinations and ionizations at a sub-grid level on a density field in a 1024³ box with sides 1.6 Gpc. The simulations have two runs to bracket the potential reionization parameter space: FAINT GALAXIES, where ionization sources are primarily low mass galaxies, producing reionization morphologies characterized by small HII patches; and BRIGHT GALAXIES, where reionization is dominated by more massive galaxies, producing larger HII patches. We use the fiducial FAINT GALAXIES, but show in Section 3.1 our results do not significantly depend on the choice of simulation run.

We populate dark matter halos in the simulations with physically motivated galaxy properties: UV luminosities from the Mason et al. (2015) model; and emitted Ly α rest-frame equivalent widths (EW) and Ly α line velocity offsets from source galaxies’ systemic redshifts, Δv . We use the empirical model presented by M18 where Δv is correlated with halo mass to encompass the complex ISM radiative transfer. Massive halos have higher Δv , likely due to increased scattering in their denser ISM (Figure 1, right panel). We model lines as Gaussians, centered at Δv , with $FWHM = \Delta v$ (for $\Delta v < 20 \text{ km s}^{-1}$ we set $FWHM = 20 \text{ km s}^{-1}$, comparable to the maximum expected thermal broadening). We assume the observed $z \sim 6$ Ly α EW distribution, $p(EW_{\text{Ly}\alpha})$, is equivalent to the emitted $z \sim 7$ $p(EW_{\text{Ly}\alpha}^{\text{emit}})$ (i.e. the change observed between these redshifts is due to reionization only) and use a $p(EW_{\text{Ly}\alpha}|M_{\text{UV}})$ fit to the $z \sim 6$ sample presented by De Barros et al. (2017) (the fit is described by M18, and accounts for Ly α non-detections).

A key quantity we compute is the differential *trans-*

mission fraction of Ly α photons through the IGM: $\mathcal{T}_{\text{IGM}}(\bar{x}_{\text{HI}}) = EW(\bar{x}_{\text{HI}})/EW(\bar{x}_{\text{HI}} = 0)$. We calculate \mathcal{T}_{IGM} by modeling the emitted Ly α lineshape and attenuating it with the damping wing absorption optical depth (τ_{IGM}) from cosmic neutral hydrogen patches along the line of sight in the simulations:

$$\mathcal{T}_{\text{IGM}}(\bar{x}_{\text{HI}}, M_h, \Delta v) = \int_0^\infty dv J_\alpha(\Delta v, M_h, v) e^{-\tau_{\text{IGM}}(\bar{x}_{\text{HI}}, M_h, v)} \quad (1)$$

where $J_\alpha(\Delta v, M_h, v)$ is the normalized Ly α lineshape emitted from galaxies. We model circumgalactic medium (CGM) absorption by truncating the lineprofiles at the halo circular velocity. As we are only interested in the differential evolution of EW this is valid assuming the only significant change in the optical depth to Ly α between $z \sim 6$ and $z \sim 7$ is due to reionization. We discuss the impact of an evolving CGM in Section 4.

We calculate \mathcal{T}_{IGM} for millions of realizations of model galaxies along thousands of sightlines in 40 $z = 7$ IGM simulation cubes with average neutral fractions $0 \leq \bar{x}_{\text{HI}} \leq 0.95$ ($\Delta\bar{x}_{\text{HI}} \sim 0.02$) to generate $p(\mathcal{T}_{\text{IGM}}|\bar{x}_{\text{HI}}, M_h)$ and forward-model the observed $p(EW_{\text{Ly}\alpha})$.

3. Results

Here we describe the key results of our study: Ly α from UV bright galaxies in massive halos can have high transmission through the IGM, even in a highly neutral universe (Section 3.1); our model is consistent with the observed evolution of the Ly α fraction, except for extremely bright galaxies ($M_{\text{UV}} \lesssim -22$) which must have higher than expected emitted Ly α EWs (Section 3.2); and UV bright galaxies can measure \bar{x}_{HI} if their emitted Ly α EW distribution is known (Section 3.3).

3.1. Boosted transmission of Ly α from massive halos

To explore the differences between the most biased galaxies and the bulk of the high redshift galaxy population we examine $p(\mathcal{T}_{\text{IGM}})$ in two halo mass bins: $10^{11.5} \leq$

¹ <http://homepage.sns.it/mesinger/EOS.html>

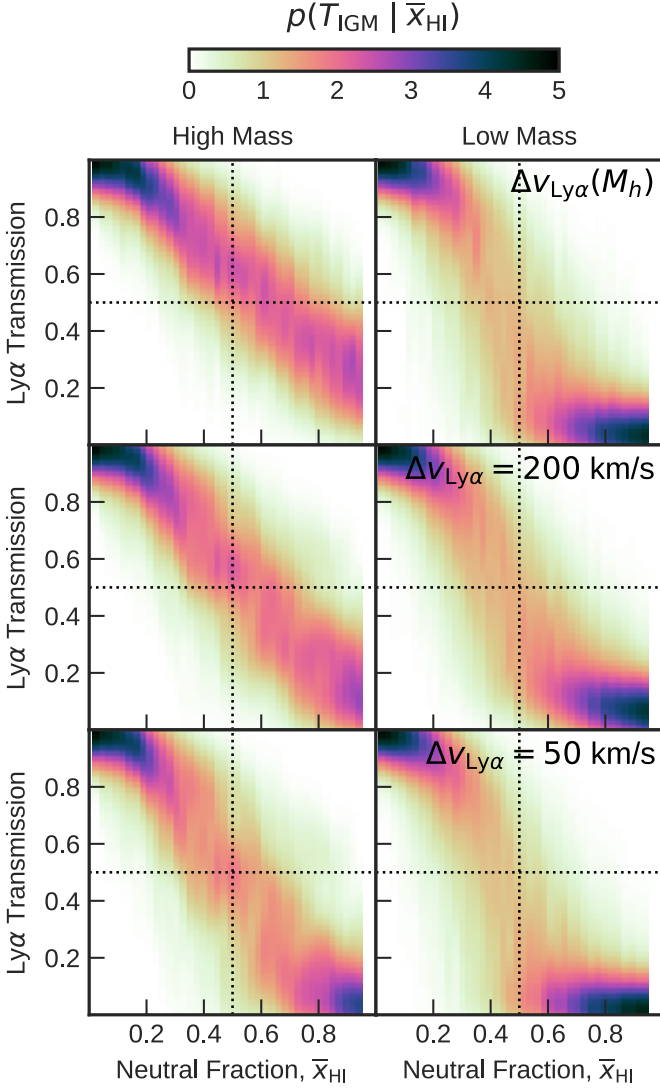


FIG. 2.— Ly α transmission fraction distributions, $p(\mathcal{T}_{\text{IGM}})$ at a given \bar{x}_{HI} . Highest density/darkest regions correspond to most likely values of \mathcal{T}_{IGM} at each \bar{x}_{HI} . We show $p(\mathcal{T}_{\text{IGM}})$ in two mass bins ($10^{11.5} \leq M_h \leq 10^{12} M_\odot$, left; $10^{10} \leq M_h \leq 10^{11} M_\odot$, right). We use three models for emitted Ly α lines: (upper panels) the mass-dependent model presented by M18, with high mass halos having higher Δv ; (middle) $\Delta v = 200 \text{ km s}^{-1}$; (lower) $\Delta v = 50 \text{ km s}^{-1}$. With mass-dependent velocity offsets \mathcal{T}_{IGM} is boosted for high mass halos.

$M_h \leq 10^{12} M_\odot$ (57 sightlines in the EoS simulations, hosting $M_{\text{UV}} \lesssim -21$ galaxies) and $10^{10} \leq M_h \leq 10^{11}$ ($\sim 10^4$ sightlines, $M_{\text{UV}} \gtrsim -19.5$ galaxies, comparable to the faintest $z > 6$ LBGs with detected Ly α , e.g. Huang et al. 2016; Hoag et al. 2017).

Figure 2 shows $p(\mathcal{T}_{\text{IGM}}|\bar{x}_{\text{HI}}, M_h)$, using three models for Ly α velocity offsets: (1) drawn from the M18 $p(\Delta v|M_h)$ model: low mass halos have median $\Delta v \sim 90 \text{ km s}^{-1}$, high mass halos have median $\Delta v \sim 220 \text{ km s}^{-1}$. (2) $\Delta v = 200 \text{ km s}^{-1}$, often the fiducial value used in reionization Ly α modeling (e.g., Dijkstra et al. 2011; Mesinger et al. 2015). (3) $\Delta v = 50 \text{ km s}^{-1}$.

Irrespective of emitted line properties, galaxies in massive halos have higher \mathcal{T}_{IGM} , as they preferentially live in overdensities which reionize early (e.g., McQuinn et al. 2007), so their Ly α photons are redshifted into the flat-

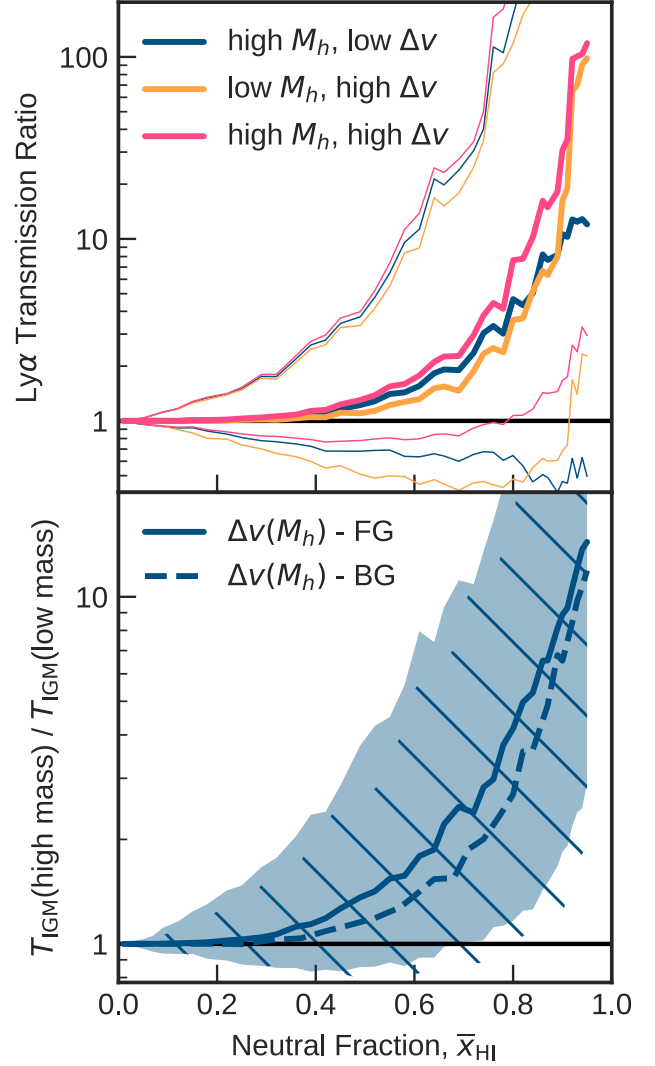


FIG. 3.— **Upper:** Ratio of \mathcal{T}_{IGM} comparing galaxies in low mass halos with $\Delta v = 50 \text{ km s}^{-1}$ with galaxies in: high mass halos, $\Delta v = 50 \text{ km s}^{-1}$ (blue); low mass halos, $\Delta v = 200 \text{ km s}^{-1}$ (orange); high mass halos, $\Delta v = 200 \text{ km s}^{-1}$ (pink). We use $p(\mathcal{T}_{\text{IGM}})$ and mass bins from Figure 2. We plot median ratios as solid thick lines and 16 – 84% range (due to sightline-to-sightline variations) as thin solid lines. The biggest boost is for galaxies in massive halos with high Δv . **Lower:** Ratio of \mathcal{T}_{IGM} for galaxies in low and high mass bins, assuming mass-dependent Δv . We show the ratio derived using the two EoS simulation runs: the fiducial FAINT GALAXIES (median - solid line, 16 – 84% - shaded region); BRIGHT GALAXIES (median - dashed line, 16 – 84% - hashed region). \mathcal{T}_{IGM} boosting in massive halos is relatively insensitive to simulation choice.

test part of the damping wing (Figure 1) by the time they reach cosmic neutral patches. Mass-dependent velocity offsets enhance this effect: Ly α from low mass halos is more easily attenuated as they have low Δv , whereas \mathcal{T}_{IGM} from massive halos is boosted.

The scatter in \mathcal{T}_{IGM} is lower for massive halos: the smaller scatter in distance from source galaxies to the first neutral patch (Figure 1) reduces the sightline-to-sightline variation in optical depths. This makes galaxies in massive halos accurate probes of \bar{x}_{HI} . The effect is most pronounced for $0.3 \lesssim \bar{x}_{\text{HI}} \lesssim 0.6$, when neutral patches are narrower and more widely separated (Mesinger & Furlanetto 2008). As noted by Mesinger & Furlanetto (2008) (though in the context of quasars), if halo masses can be

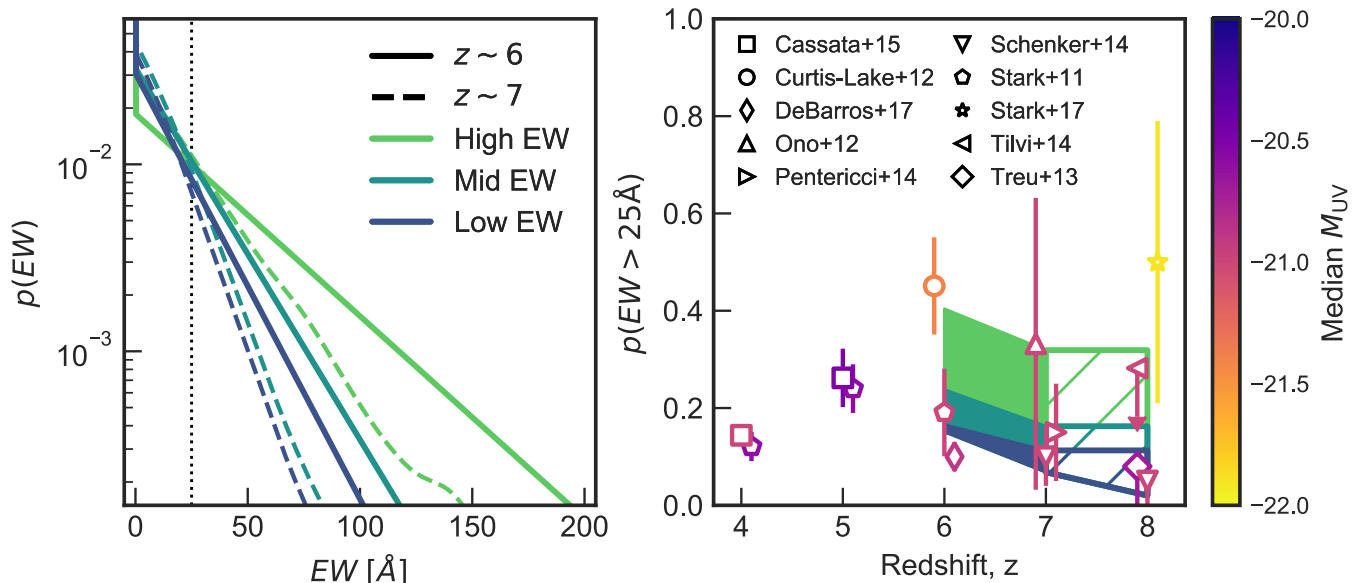


FIG. 4.— Redshift evolution of $p(EW_{\text{Ly}\alpha})$ for galaxies in massive halos, for three model $p(EW_{\text{Ly}\alpha})$ (Low, Mid and High). **Left:** Each $p(EW_{\text{Ly}\alpha})$ model at $z \sim 6$ (solid, fit from De Barros et al. 2017) and $z \sim 7$ (dashed, assuming the inferred median $\bar{x}_{\text{HI}} = 0.59$ by M18). **Right:** The fraction of LBGs showing $\text{Ly}\alpha$ $EW > 25\text{\AA}$ (dotted black line in left panel). We plot observations of UV bright samples (indicated by point shape, Stark et al. 2011; Curtis-Lake et al. 2012; Ono et al. 2012; Treu et al. 2013; Tilvi et al. 2014; Pentericci et al. 2014; Schenker et al. 2014; Cassata et al. 2015; Stark et al. 2017; De Barros et al. 2017), with the samples’ median M_{UV} indicated by color. Shaded regions show the range of evolution allowed by the M18 \bar{x}_{HI} constraints (16 – 84% range), for a given model $p(EW_{\text{Ly}\alpha})$. Hashed regions indicate the allowed evolution to $z = 8$ assuming \bar{x}_{HI} does not increase.

estimated for galaxies the accuracy in \bar{x}_{HI} increases.

The top panel of Figure 3 investigates contributions to \mathcal{T}_{IGM} . We compare \mathcal{T}_{IGM} from galaxies in low and high mass halos, with fixed low or high Δv , to galaxies in low mass halos with low Δv . Massive halos always have high \mathcal{T}_{IGM} , as they reside in larger ionized bubbles, indicating halo mass is the dominant cause of high transmission. When $\text{Ly}\alpha$ is emitted at high Δv \mathcal{T}_{IGM} is significantly boosted for massive halos. In the very early stages of reionization \mathcal{T}_{IGM} is boosted for low mass halos with high Δv compared to low Δv , massive halos, likely because ionized bubbles around massive halos are still small.

The lower panel of Figure 3 shows a realistic estimate of the boosting, using mass-dependent Δv (comparing the top panels of Figure 2). For $\bar{x}_{\text{HI}} > 0.6$ \mathcal{T}_{IGM} for massive halos are $> 2\times$ higher than for low mass halos, rising to a factor ~ 10 for $\bar{x}_{\text{HI}} > 0.9$. We compare the transmission ratio for the two EoS simulations: FAINT GALAXIES and BRIGHT GALAXIES (Section 2). The transmission boost is comparable; this effect is relatively independent of the timeline and morphology of reionization. We use these realistic \mathcal{T}_{IGM} for UV bright galaxies in the next sections.

3.2. Evolving Ly α fraction for UV bright galaxies

An increasing fraction of $\text{Ly}\alpha$ emitters ($EW > 25\text{\AA}$) is observed in the LBG population over $2 \lesssim z \lesssim 6$ (e.g., Stark et al. 2010; Cassata et al. 2015), likely due to decreasing dust in galaxies (Hayes et al. 2011). A drop in the $\text{Ly}\alpha$ fraction at $z > 6$ is usually attributed to absorption by an increasingly neutral IGM during reionization (see Dijkstra 2014, for a recent review).

Figure 4 (right panel) shows the $4 \leq z \leq 8$ $\text{Ly}\alpha$ fraction for UV bright galaxies. At $z < 6$ the observations are consistent, but at $z \geq 6$ the $\text{Ly}\alpha$ fraction measured for samples with $M_{\text{UV}} \lesssim -21.5$ (Curtis-Lake et al. 2012; Stark et al. 2017) is significantly higher than for those at

lower luminosities. Much of this discrepancy may be due to selection effects: using only the z_{850} -band for LBG selection the Curtis-Lake et al. (2012) sample could be biased towards strong $\text{Ly}\alpha$ emission (De Barros et al. 2017), and the Stark et al. (2017) sample was selected via red Spitzer/IRAC [3.6]-[4.5] colors (Roberts-Borsani et al. 2016) making them likely strong [OIII]+H β emitters, requiring hard radiation fields and young stellar populations, which increase $\text{Ly}\alpha$ production and escape (Finkelstein et al. 2013; Zitrin et al. 2015). Using our model we test how the boosted \mathcal{T}_{IGM} for galaxies in massive halos (Section 3.1) contributes to their $\text{Ly}\alpha$ emitter fraction.

We plot the evolution allowed by the M18 $z \sim 7$ neutral fraction estimate ($\bar{x}_{\text{HI}} = 0.59^{+0.11}_{-0.15}$) for galaxies in massive halos, using the maximum transmission demonstrated in Figure 2 (top left panel). We forward-model $p(EW_{\text{Ly}\alpha}^{\text{obs}})$ by convolving $p(\mathcal{T}_{\text{IGM}})$ with the UV magnitude-dependent $p(EW_{\text{Ly}\alpha}^{\text{emit}})$ described in Section 2. $p(EW_{\text{Ly}\alpha}^{\text{emit}})$ is a major uncertainty so we use a range of distributions: LOW-EW, MID-EW and HIGH-EW, corresponding to the measured $z \sim 6$ distributions for LBGs with $M_{\text{UV}} \sim \{-21, -20.5, -20\}$, which bracket the EW variation in the De Barros et al. (2017) sample (Figure 4, left panel). Based on $z \leq 6$ observations we expect UV bright galaxies to have LOW-EW or MID-EW distributions.

The observed evolution of the $\text{Ly}\alpha$ fraction for $M_{\text{UV}} > -21.5$ samples is consistent with negligible evolution in $p(EW_{\text{Ly}\alpha}^{\text{emit}})$. The HIGH-EW distribution is required to be consistent with the Stark et al. (2017) $\text{Ly}\alpha$ fraction error region, which is unexpected given UV bright galaxies at lower redshifts tend to have low $\text{Ly}\alpha$ EWs (e.g., Stark et al. 2010).

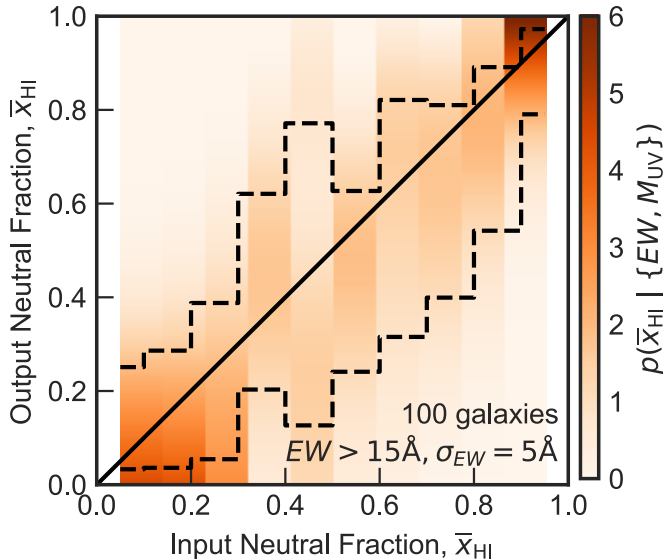


FIG. 5.— Posterior distributions for \bar{x}_{HI} for a grid of input \bar{x}_{HI} using simulated samples of 100 $M_{\text{UV}} = -22$ galaxies. Each vertical strip is a posterior for input \bar{x}_{HI} , darkest colors show the highest probabilities. The one-to-one relation between input and output \bar{x}_{HI} is shown as a solid black line. We plot the 16 – 84% range for each posterior (within dashed lines). The posteriors are consistent with the input \bar{x}_{HI} within this range.

3.3. UV bright galaxies as probes of reionization

To test the efficacy of UV bright galaxies as probes of reionization we perform a Bayesian inference to obtain the posterior distribution of the neutral fraction given simulated observations of galaxies with Ly α EW and M_{UV} measurements: $p(\bar{x}_{\text{HI}} | \{EW_{\text{Ly}\alpha}, M_{\text{UV}}\})$. Using Bayes’ theorem this posterior is proportional to $\prod_i p(EW_{\text{Ly}\alpha,i} | \bar{x}_{\text{HI}}, M_{\text{UV},i}) \times p(\bar{x}_{\text{HI}})$, assuming the observations are independent.

We follow the method described by M18 and generate the likelihood of observing a given EW: $p(EW_{\text{Ly}\alpha} | \bar{x}_{\text{HI}}, M_{\text{UV}})$, by convolving the high halo mass $p(\mathcal{T}_{\text{IGM}})$, described in Section 3.1, with a distribution of emitted EWs. For this work we consider $M_{\text{UV}} = -22$ galaxies. By assigning galaxies to a range of halo masses we include some scatter in $M_h - M_{\text{UV}}$ (e.g., Finkelstein et al. 2015). To generate mock observations we draw EW values from a likelihood for a given \bar{x}_{HI} , convolve with a 5\AA uncertainty and treat galaxies with $EW < 15\text{\AA}$ as non-detections (which are robustly accounted for in the inference). We perform the inference using these mock observations.

Figure 5 shows the posteriors obtained using a simulated sample of 100 UV bright galaxies for a grid of input \bar{x}_{HI} values. The inferred posteriors are consistent with the input values over the entire range within the 16 – 84% region, showing UV bright galaxies can be accurate tracers of the average IGM state. We note our posteriors are broad ($\Delta\bar{x}_{\text{HI}} \sim 0.4$) compared to those obtained using fainter galaxies (c.f. $\Delta\bar{x}_{\text{HI}} \sim 0.25$ in M18). This uncertainty is driven by the shape of $p(EW_{\text{Ly}\alpha})$, which declines with increasing EW. Reionization further kills the high EW tail of the distribution, making high EW objects rare.

4. Discussion

We have shown UV bright galaxies in high mass halos can be precise probes of reionization and are increasingly valuable in reionization’s early stages when Ly α in UV faint galaxies, emitted close to systemic velocity, is overwhelmingly absorbed in the IGM. However, there are two limitations to using such galaxies to probe reionization: (1) they are rare; (2) they emit less Ly α due to absorption in their dense ISM. Below we discuss prospects for overcoming these limitations.

Wide-area photometric surveys such as the Brightest of Reionizing Galaxies survey (BoRG, Trenti et al. 2011), UltraVISTA and UDS (e.g., Bowler et al. 2015) and GOLDRUSH (Ono et al. 2018) have discovered ~ 100 $z \gtrsim 7$ $M_{\text{UV}} \lesssim -21$ LBGs in $\sim 100 \text{ deg}^2$. Future wide-area surveys with e.g., *WFIRST* (Spergel et al. 2013) and *Euclid* (Laureijs et al. 2011) will likely increase this by a factor $\gtrsim 100$ in $> 15,000 \text{ deg}^2$. These sources will be ideal candidates for spectroscopic follow-up to measure the Ly α EW distribution needed to infer the neutral fraction.

Do UV bright galaxies emit less Ly α ? Whilst most $z \lesssim 6$ observations indicate they do (e.g., Verhamme et al. 2008; Stark et al. 2010), our results suggest the $z \sim 8$ galaxies presented by Stark et al. (2017) must have high intrinsic Ly α EW. Recent observations of a $M_{\text{UV}} \sim -22$ galaxy after reionization at $z \sim 4$ detected Ly α emission with low Δv and Lyman continuum radiation (Vanzella et al. 2018), suggesting significantly ionized pathways through the ISM and/or CGM from such galaxies. If these galaxies are efficient producers of ionizing radiation, they may also increase their local ionization field to boost Ly α transmission through the CGM/IGM.

A holistic understanding of Ly α emission as a function of redshift and galaxy properties is therefore crucial to improve the use of Ly α as a cosmological tool. These measurements are becoming increasingly feasible with multi-wavelength observations of LBGs, and time should be invested in establishing Ly α emission properties over a wide redshift and galaxy mass/UV magnitude range, both in wide areas, and in deep lensed fields with *HST* (e.g., Treu et al. 2015; Schmidt et al. 2016) and in the near future with *JWST* (Treu et al. 2017). Better measurements of these properties will enable us to disentangle IGM, CGM and ISM effects.

5. Summary and Conclusions

We have investigated the IGM transmission of Ly α from UV bright galaxies during the Epoch of Reionization by combining reionization simulations and empirical relations for galaxy and Ly α properties. Our main conclusions are:

- (i) Ly α emitted by UV bright galaxies in massive halos has a higher mean and lower dispersion in IGM transmission than Ly α from typical field galaxies in low mass halos. This is primarily due to massive halos predominantly residing in overdensities which reionize early, and boosted by their higher Ly α velocity offsets, reducing damping wing absorption by cosmic neutral hydrogen.
- (ii) This boosted transmission is not sufficient to explain the observed evolution of the $6 \lesssim z \lesssim 8$ Ly α

fraction for extremely UV bright galaxies (Stark et al. 2017), suggesting these objects have higher emitted Ly α EW than expected.

- (iii) With sufficient numbers, the observed Ly α EW distribution of UV bright galaxies can place tight constraints on the IGM neutral fraction during reionization, and may be the only way to probe the IGM at $z > 7$ when quasars are exceedingly rare and Ly α from most UV faint galaxies is extinguished.

More comprehensive measurements of the Ly α EW distribution as a function of redshift and galaxy properties are necessary to understand the evolving visibility of Ly α emission and to disentangle the effects of the ISM and IGM during reionization. Current and upcoming spec-

troscopic observations have the ability to this and increase the efficacy of Ly α as a cosmological tool.

We thank Dan Stark and Crystal Martin for useful discussions. CM acknowledges support through the NASA Earth and Space Science Fellowship Program Grant NNX16AO85H. AM acknowledges European Research Council support under the European Union's Horizon 2020 research and innovation program (grant No 638809 - AIDA). MT acknowledges support by the Australian Research Council (awards FT130101593 and CE170100013). This work was supported by *HST* BoRG grants GO-12572, 12905, 13767 and 15212, and *HST* GLASS grant GO-13459.

Software: IPython (Pérez & Granger 2007), matplotlib (Hunter 2007), NumPy (Van Der Walt et al. 2011), and EMCEE (Foreman-Mackey et al. 2013).

REFERENCES

- Bañados, E., Venemans, B. P., Mazzucchelli, C., et al. 2017, *Nature*, **553**, 473
- Barone-Nugent, R. L., Trenti, M., Wyithe, J. S. B., et al. 2014, *ApJ*, **793**, 17
- Bowler, R. A. A., Dunlop, J. S., McLure, R. J., et al. 2015, *MNRAS*, **452**, 1817
- Cassata, P., Tasca, L. A. M., Le Fèvre, O., et al. 2015, *A&A*, **573**, A24
- Castellano, M., Dayal, P., Pentericci, L., et al. 2016, *ApJ*, **818**, L3
- Curtis-Lake, E., McLure, R. J., Pearce, H. J., et al. 2012, *MNRAS*, **422**, 1425
- De Barros, S., Pentericci, L., Vanzella, E., et al. 2017, *A&A*, **608**, A123
- Dijkstra, M. 2014, *PASA*, **31**, e040
- Dijkstra, M., Mesinger, A., & Wyithe, J. S. B. 2011, *MNRAS*, **414**, 2139
- Finkelstein, S. L., Papovich, C., Dickinson, M., et al. 2013, *Nature*, **502**, 524
- Finkelstein, S. L., Song, M., Behroozi, P., et al. 2015, *ApJ*, **814**, 95
- Fontana, A., Vanzella, E., Pentericci, L., et al. 2010, *ApJ*, **725**, L205
- Foreman-Mackey, D., Hogg, D. W., Lang, D., & Goodman, J. 2013, *PASP*, **125**, 306
- Greig, B., Mesinger, A., Haiman, Z., & Simcoe, R. A. 2016, *MNRAS*, **466**, 4239
- Hayes, M., Schaerer, D., Östlin, G., et al. 2011, *ApJ*, **730**, 8
- Hoag, A., Bradač, M., Trenti, M., et al. 2017, *Nature Astronomy*, **1**, 0091
- Huang, K.-H., Lemaux, B. C., Schmidt, K. B., et al. 2016, *ApJ*, **823**, L14
- Hunter, J. D. 2007, *Comput. Sci. Eng.*, **9**, 99
- Laureijs, R., Amiaux, J., Arduini, S., et al. 2011, *arXiv:1110.3193*
- Mason, C. A., Trenti, M., & Treu, T. 2015, *ApJ*, **813**, 21
- Mason, C. A., Treu, T., Dijkstra, M., et al. 2018, *ApJ*, **856**, 2
- McQuinn, M., Lidz, A., Zahn, O., et al. 2007, *MNRAS*, **377**, 1043
- Mesinger, A., Aykutaalp, A., Vanzella, E., et al. 2015, *MNRAS*, **446**, 566
- Mesinger, A., & Furlanetto, S. R. 2008, *MNRAS*, **385**, 1348
- Mesinger, A., Greig, B., & Sobacchi, E. 2016, *MNRAS*, **459**, 2342
- Oesch, P. A., Dokkum, P. G. V., Illingworth, G. D., et al. 2015, *ApJ*, **804**, L30
- Ono, Y., Ouchi, M., Mobasher, B., et al. 2012, *ApJ*, **744**, 83
- Ono, Y., Ouchi, M., Harikane, Y., et al. 2018, *PASJ*, **70**, S10
- Pentericci, L., Vanzella, E., Fontana, A., et al. 2014, *ApJ*, **793**, 113
- Pérez, F., & Granger, B. E. 2007, *Comput. Sci. Eng.*, **9**, 21
- Planck Collaboration, Adam, R., Ade, P. A. R., et al. 2015, *A&A*, **594**, A8
- Roberts-Borsani, G. W., Bouwens, R. J., Oesch, P. A., et al. 2016, *ApJ*, **823**, 143
- Schenker, M. A., Ellis, R. S., Konidaris, N. P., & Stark, D. P. 2014, *ApJ*, **795**, 20
- Schmidt, K. B., Treu, T., Bradač, M., et al. 2016, *ApJ*, **818**, 38
- Spergel, D., Gehrels, N., Breckinridge, J., et al. 2013, *arXiv:1305.5422*
- Stark, D. P., Ellis, R. S., Chiu, K., Ouchi, M., & Bunker, A. 2010, *MNRAS*, **408**, 1628
- Stark, D. P., Ellis, R. S., & Ouchi, M. 2011, *ApJ*, **728**, L2
- Stark, D. P., Ellis, R. S., Charlot, S., et al. 2017, *MNRAS*, **464**, 469
- Tilvi, V., Papovich, C., Finkelstein, S. L., et al. 2014, *ApJ*, **794**, 5
- Trenti, M., Bradley, L. D., Stiavelli, M., et al. 2011, *ApJ*, **727**, L39
- , 2012, *ApJ*, **746**, 55
- Treu, T., Schmidt, K. B., Trenti, M., Bradley, L. D., & Stiavelli, M. 2013, *ApJ*, **775**, L29
- Treu, T., Schmidt, K. B., Brammer, G. B., et al. 2015, *ApJ*, **812**, 114
- Treu, T., Abramson, L., Bradac, M., et al. 2017, Through the Looking GLASS: A JWST Exploration of Galaxy Formation and Evolution from Cosmic Dawn to Present Day, *JWST Proposal ID 1324. Cycle 0 Early Release Science*
- Van Der Walt, S., Colbert, S. C., & Varoquaux, G. 2011, *Comput. Sci. Eng.*, **13**, 22
- Vanzella, E., Nonino, M., Cupani, G., et al. 2018, *MNRAS*, **476**, 15
- Verhamme, A., Schaerer, D., Atek, H., & Tapken, C. 2008, *A&A*, **491**, 89
- Zitrin, A., Labbé, I., Belli, S., et al. 2015, *ApJ*, **810**, L12